

Preparation of Polymer-Stabilized Magnetic Iron Oxide as Selective Drug Nanocarriers to Human Acute Myeloid Leukemia

Kheireddine El-Boubbou

Abstract—Drug delivery to target human acute myeloid leukemia (AML) using a nanoparticulate chemotherapeutic formulation that can deliver drugs selectively to AML cancer is hugely needed. In this work, we report the development of a nanoformulation made of polymeric-stabilized multifunctional magnetic iron oxide nanoparticles (PMNP) loaded with the anticancer drug Doxorubicin (Dox) as a promising drug carrier to treat AML. Dox@PMNP conjugates simultaneously exhibited high drug content, maximized fluorescence, and excellent release properties. Nanoparticulate uptake and cell death following addition of Dox@PMNPs were then evaluated in different types of human AML target cells, as well as on normal human cells. While the unloaded MNPs were not toxic to any of the cells, Dox@PMNPs were found to be highly toxic to the different AML cell lines, albeit at different inhibitory concentrations (IC_{50} values), but showed very little toxicity towards the normal cells. In comparison, free Dox showed significant potency concurrently to all the cell lines, suggesting huge potentials for the use of Dox@PMNPs as selective AML anticancer cargos. Live confocal imaging, fluorescence and electron microscopy confirmed that Dox is indeed delivered to the nucleus in relatively short periods of time, causing apoptotic cell death. Importantly, this targeted payload may potentially enhance the effectiveness of the drug in AML patients and may further allow physicians to image leukemic cells exposed to Dox@PMNPs using MRI.

Keywords—Magnetic nanoparticles, drug delivery, acute myeloid leukemia, iron oxide, cancer nanotherapy.

I. INTRODUCTION

DRUG delivery systems are receiving immense attention for pharmaceutical and biomedical applications due to their potential to improve therapeutic targeting, enhance the drug efficacy, and reduce the systemic side effects of chemotherapeutic drugs [1], [2]. Recently, innovative therapeutic approaches beyond the conventional therapies of using chemical drugs are being actively developed [3], [4]. Of the many varieties, magnetic iron oxide nanoparticles (MNPs) have been widely popularized not only as magnetic imaging vehicles, but also as drug nanocarriers [5]-[8]. Hence, MNPs are excellent candidates for targeted drug delivery and image-guided therapeutics with a great potential in clinical cancer theranostics [9]. Although there are various reports on the utilization of drug-loaded superparamagnetic iron oxide

nanoparticles for cancer imaging and therapy [10], [11], very few reports have focused on human AML [12].

AML is a devastating acute cancer caused by the replacement of normal blood cells with leukemic cells, with limited treatment strategies possibly due to poorly effective drug delivery to affected areas [13]. Unlike solid tumors, AML cannot be cured by surgical treatment. The main strategy is to treat it using chemotherapy. Dox is one of the most studied chemotherapeutic anticancer drugs used for the treatment of a wide range of hematological malignancies (i.e. leukemia and lymphoma) in clinical practice [14]-[17]. However, the cardiotoxicity and poor selectivity of this drug limits its cumulative dosage to effective levels resulting in off-target side effects. Hence, there is a great incentive to develop alternative, rapid and more effective chemotherapeutic approaches to treat AML.

In this work, a chemotherapeutic formulation made of polymer-stabilized MNPs of ferrites loaded with the anticancer drug Dox was developed, and its cytotoxic effects on a panel of different AML leukemic cells was explored. The utilization of the prepared drug-loaded MNPs as effective delivery vehicles for different types of AML cells were evaluated. Importantly, the MNP formulation developed here can potentially open new opportunities for *in vivo* AML therapeutic imaging and hyperthermia.

II. RESULTS AND DISCUSSION

Dox@PMNPs were prepared according to our previously published work [18], [19] *via* the Ko-precipitation Hydrolytic Basic (KHB) method, producing stable colloidal formulation of desirable size dispersed in aqueous media (Fig. 1). Non covalent chemistry was then chosen to adsorb Dox onto MNPs, as it has the advantage to preserve the structure of the NPs and, thus, their unique properties and intracellular tracking.

Dox@PMNPs obtained were thoroughly characterized by a variety of techniques including transmission electron microscope (TEM), dynamic light scattering (DLS), and thermal gravimetric analyses (TGA) (Fig. 2). Respective TEM image of a typical Dox@PMNP dried sample clearly shows ~ 5 nm – 10 nm sized NPs. DLS measurements of an aqueous dispersion of Dox@PMNPs in water revealed a hydrodynamic size (D_H) = ~ 150 nm with a uniform and narrow size distribution of the as-synthesized particles. No significant changes in the size were observed with time, further confirming the remarkable stability of the particles in their

Kheireddine El-Boubbou is with the King Saud bin Abdulaziz University for Health Sciences, King Abdulaziz Medical City, National Guard Health Affairs, Riyadh 11481, Saudi Arabia and King Abdullah International Medical Research Center (KAIMRC), National Guard Hospital, Riyadh 11426, Saudi Arabia (e-mail: elboubboukh@ngha.med.sa).

aqueous dispersions. Furthermore, TGA showed ~ 35 % weight loss of Dox-loaded PMNPs, further confirming the

successful adsorption of Dox onto the PMNPs.

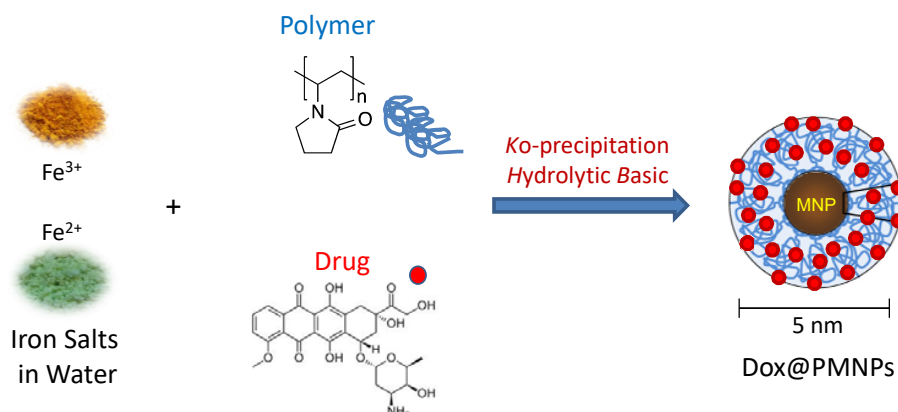


Fig. 1 Schematic illustration for the preparation of Dox@PMNPs

Finally, our studies demonstrated that the simple non-covalent approach chosen allowed the formation of colloidal water-dispersible drug-loaded PMNP formulations with good loading efficiencies. Between 40% - 60% of the drug can be loaded onto PMNPs (i.e. 60 μg of Dox/mg PMNPs in this case), depending on the concentration of Dox added.

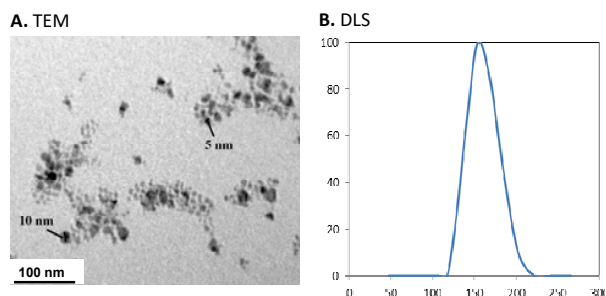


Fig. 2 Characterization of Dox@PMNPs. A) TEM image of dried NP sample (the core NP sizes = 5 - 10 nm); B) DLS measurement of Dox@PMNPs dispersed in water showing $D_H = 150$ nm

With the MNPs in hand, we first investigated the uptake of the NPs by the different cell lines by Fluorescence Activated Cell Sorting (FACS) cytometry. We, thus, labeled the NPs with a fluorescent label fluorescein, and then incubated AML cells with the labeled PMNPs (10 $\mu\text{g}/\text{mL}$). All cell lines tested showed a significant increase in cell fluorescence, as early as 15 minutes post-incubation with the labeled NPs, compared to control cells or to cells treated with unlabeled PMNPs (Fig. 3). Mean fluorescence intensity of cells seemed to increase over time, with no significant changes after 6 hrs. This indicates that Dox@PMNPs start being taken up by AML cells, minutes following incubation and the uptake continues up to 24 hrs, implying that the major route of Dox delivery is through endocytic uptake of Dox@PMNPs into the cell followed by the intracellular release of Dox rather than extracellular release of Dox at the cell surface. No significant change in the fluorescent intensity of the incubated cells was observed after

24 hrs, confirming that most of the uptake and drug release took place in the first 6 hrs. This is similar to what has been observed earlier [17]. In order to show that the observed increase in mean fluorescence reflects an early cellular uptake of NPs, and is not only due to their adherence to the cellular membrane, we also measured fluorescence signals of the incubated cells before and after washing with cell culture medium at all time-points. Although the mean fluorescence intensity decreased upon washing due to the loss of the NPs, all treated cells still showed increased fluorescence intensity as compared to the control threshold even after extensive washing, confirming that uptake of NPs does start at early time-points and increase with time.

We then sought to quantify the cytotoxicities of the MNPs towards four different AML cell lines. Dox@PMNPs were cytotoxic to all AML cell lines tested (HL-60, ML-2, and TF1-vRaf) with IC_{50} values ranging from 9 $\mu\text{g}/\text{mL}$ to 37 $\mu\text{g}/\text{mL}$ NP content corresponding to 1.1 μM to 4.6 μM Dox (Fig. 4). The IC_{50} values for ML-2, TF1-vRaf, and HL-60 were found to be 9, 28, and 37, respectively, based on the NP concentrations. Mono-Mac-1 cells can still be killed by Dox@PMNPs, albeit at higher concentrations (120 $\mu\text{g}/\text{mL}$ NP content; 15 μM Dox). These results suggest that there may be fundamental differences of immunoprofiles and morphologic changes between the various AML cell lines. Importantly, the potency of Dox@PMNPs was found to be comparable to the potency of free Dox indicating that the NP formulations are an effective vehicle for delivery of Dox to all AML cell lines. Unloaded PMNPs were not cytotoxic to any of the AML cell lines tested, even at concentrations higher than the maximal used (up to 150 $\mu\text{g}/\text{mL}$), demonstrating that the cytotoxicity of Dox@PMNPs is due exclusively to delivery of Dox to cells and not to any inherent toxicity of the NPs. We hypothesize that the observed cytotoxic effect is dependent on the uptake of NPs by cells, which after intracellular endosomal accumulation release the drug causing apoptosis and cell death.

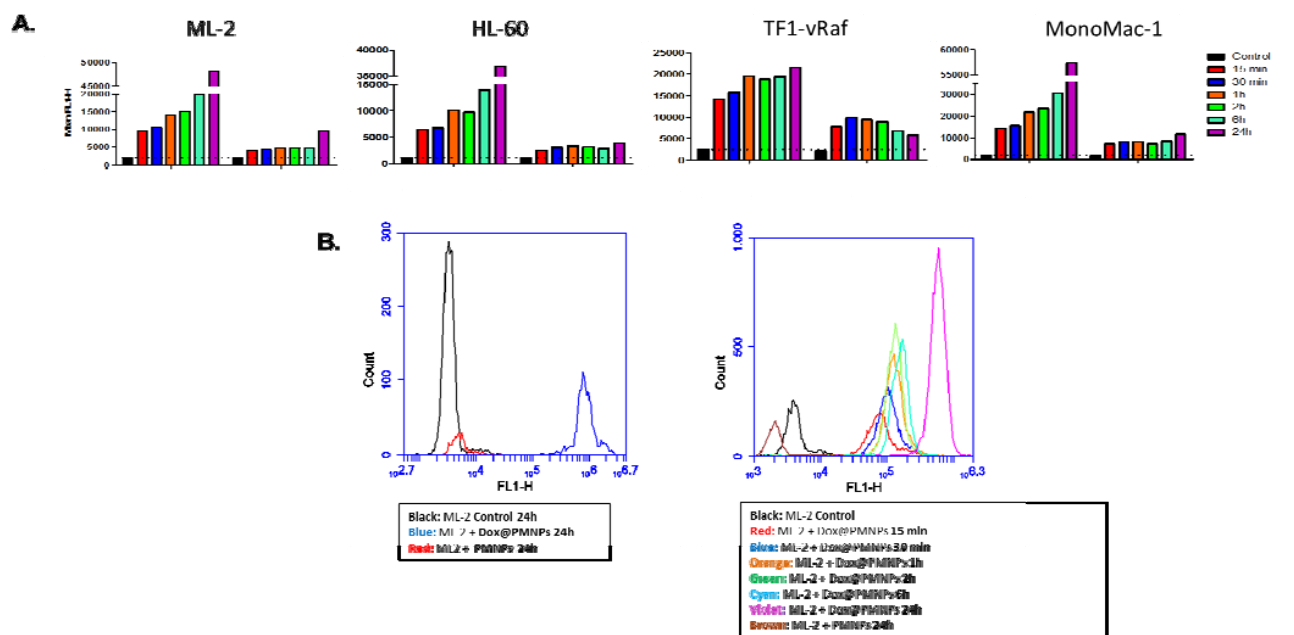


Fig. 3 (A) Quantitative flow cytometry analysis of the cellular association of the labeled Dox@PMNPs after various treatments with the four different AML cell lines ML-2, HL-60, TF1-vRaf, and Mono-Mac-1. (B) Representative intracellular fluorescence intensity of ML-2 cells analyzed by flow cytometry (The cells were gated on width versus forward scatter). All the cells were incubated with the NPs at 50 $\mu\text{g}/\text{mL}$ for 15 min, 30 min, 1 hr, 2hrs, 6 hrs and 24 hrs compared to control untreated cells. An enhanced fluorescent uptake of NPs with all the cell lines was clearly evident, even at 15 min post treatment, confirming the successful intracellular delivery due to uptake of Dox-loaded PMNPs

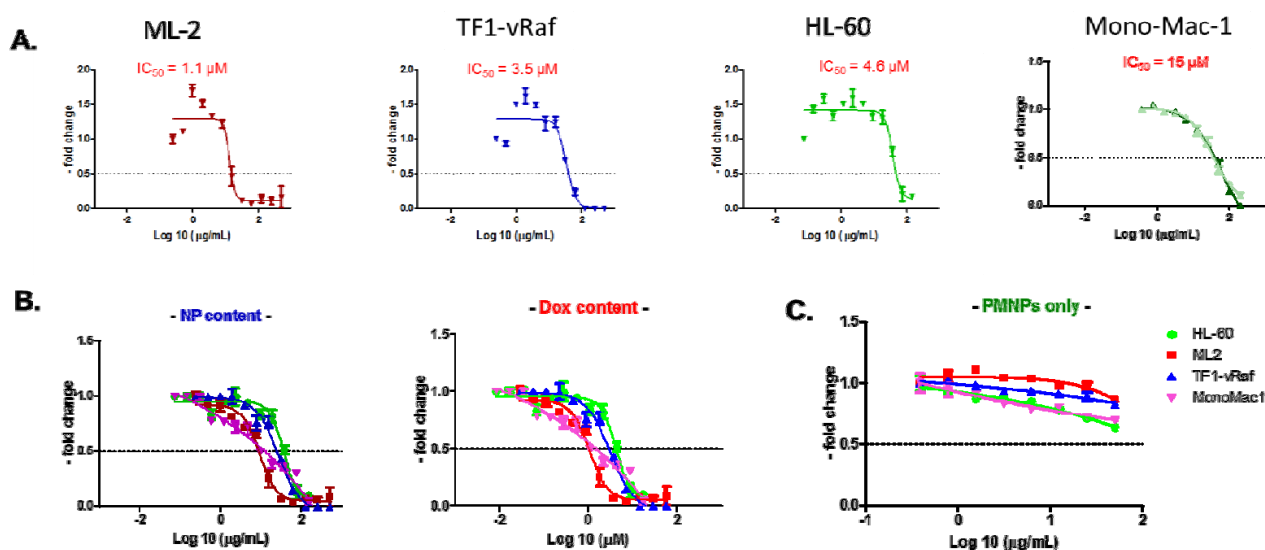


Fig. 4 (A) Non-linear regression curves of the cytotoxicity assays of Dox@PMNPs on the different AML cell lines ML-2, TF1-vRaf, HL-60, and Mono-Mac-1. The cells were incubated with different concentrations of NPs at 37°C for 48 hrs. X-axis: Log 10 of Dox content expressed in μM ; y-axis: fold change. (B) Overlay of the four curves expressed as both NP concentration and their equivalent Dox concentration. (C) Cells incubated with different concentrations of unloaded PMNPs. The unloaded PMNPs were significantly non-toxic to the AML cell lines tested, even at the highest concentrations used

In order to further confirm the intracellular distribution and localization of the NPs, confocal laser scanning microscopy (CLSM) studies were performed. Live confocal images with no fixation of cells were conducted. Our results showed that Dox is indeed delivered to the cell cytoplasm in relatively short periods of time in 1 h– 6 h and to the nucleus after

overnight incubation. The intensity of the red fluorescence increased gradually with time, resulting from the drug released from the MNPs. Interestingly, incubating the same cell lines with free Dox at equivalent concentrations, the red fluorescence was found to be directly localized in the nucleus with minimal presence in the cytoplasm (Fig. 5), as has been

observed earlier [14], [18]. It is, thus, clear that while free Dox is internalized by passive diffusion through the cell membrane, the uptake of Dox@PMNPs is rather directed by endocytic trafficking mechanisms. All these results indicate that the observed cytotoxic effects are dependent on the uptake of the NPs by cells where Dox is released and then translocated to the nucleus exerting its cytotoxic action, in relatively short periods of time. Importantly, this targeted payload is promising to enhance the effectiveness of the drug in AML patients and may further allow physicians to image the cells exposed to MNPs opening new opportunities for *in vivo* therapeutic imaging and hyperthermia.

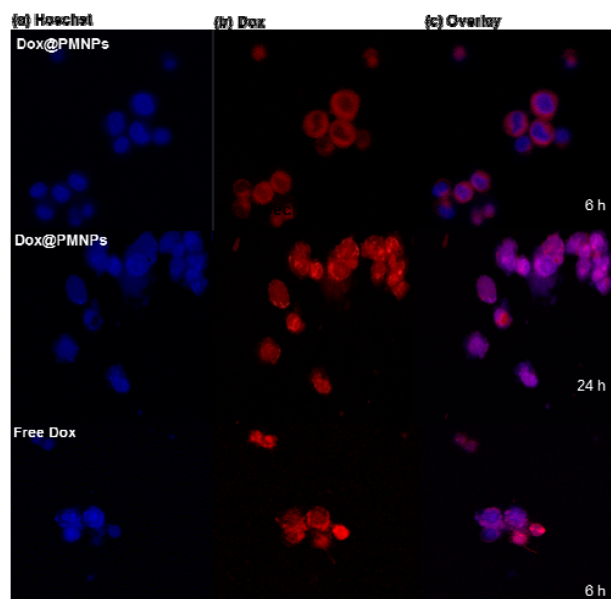


Fig. 5 Laser confocal microscopy images of representative AML cell line incubated with Dox@PMNPs (10 $\mu\text{g/mL}$ NPs; equivalent to 2.5 μM Dox) for 6 hrs or 24 hrs. (a) Blue Hoechst channel staining nuclei, (b) Red Dox channel, and (c) overlay of the images. AML cells treated with Dox alone showed Dox fluorescence diffused mostly to the nucleus, whereas NP-treated cells showed Dox signal in the cytoplasm translocating to the nucleus with time

III. CONCLUSION

We developed a chemotherapeutic nanoformulation loaded with anticancer drug as a promising drug carrier to different types of AML cells. With its superior properties, the Dox@PMNPs enabled the monitoring of NP uptake by fluorescence imaging, confocal, and electron microscopy. While PMNPs were biocompatible to cells, Dox@PMNPs were found to be highly potent to the different AML cancer cells at different inhibitory concentrations with different uptake mechanism compared to free Dox. From our results, it is clear that MNPs are endocytosed inside the cell cytoplasm, but not the nucleus, releasing the toxic drug payload to kill the cells. The prepared nano-formulation developed here can potentially open new opportunities for *in vivo* AML theranostics.

IV. MATERIALS AND METHODS

All chemicals and solvents were obtained from commercial suppliers and used as supplied. Iron (III) chloride hexahydrate ($\text{FeCl}_3 \cdot 6\text{H}_2\text{O}$), iron (II) chloride tetrahydrate ($\text{FeCl}_2 \cdot 4\text{H}_2\text{O}$), Dox, fluorescein, and the polymer Poly-N-vinylpyrrolidone (PVP) (MW = 58,000) were all purchased from UFC Biotechnology. All cell lines were purchased from the American Type Culture Collection (ATCC) and grown in RPMI 1640 medium supplemented with 10% FBS and 1% Penicillin/Streptomycin. TEM images were collected on a JEOL-JEM 1230 operating at 100 kV using Gatan camera with Digital Micrograph Imaging software. DLS measurements were assessed on Malvern Zetasizer Nano ZS instrument. TGA were carried out on a PerkinElmer TGA 4000 equipment and the samples were burned under nitrogen at a constant heating rate of $10^\circ\text{C}/\text{min}$ from 35°C to 700°C . Flow cytometry was conducted on Beckton Dickinson FACS-CANTOII. Confocal microscopy images were visualized using inverted Zeiss LSM 780 multiphoton laser scanning confocal microscope equipped with 20x and 40x (oil immersion) objectives and axiocam cameras.

Preparation of Dox@PMNPs. $\text{FeCl}_3 \cdot 6\text{H}_2\text{O}$ (40 mg, 0.15 mmol) and PVP (20 mg) were mixed in water (1 mL), followed by addition of 1 mL aqueous $\text{FeCl}_2 \cdot 4\text{H}_2\text{O}$ (15 mg, 0.075 mmol). To the above mixture, 750 μL Dox.HCl solution (0.5 mg/mL) were added, followed by addition of 2 mL NH_4OH base. The reaction mixture was stirred for 3 hrs at room temperature under inert argon atmosphere. The NP dispersion was then isolated *via* centrifugation (4500 rpm, 20 min), washed repeatedly (6x) with water until no Dox was detected in the supernatant, and finally redispersed in water to form stable aqueous suspensions of Dox@PMNPs (1 mg/mL NP; 60 $\mu\text{g/mL}$ Dox). The percentage of Dox loading (w/w%) was quantified as previously determined by UV-vis spectroscopy [19].

Uptake measurement by flow cytometry. The non-adherent AML cells (3×10^5 cells/well, 250 μL) were plated in 24-well plates overnight in their respective growth medium. The needed doses of NPs were diluted in cell culture medium as before, and added to the plates in order to reach a total volume of 500 $\mu\text{L}/\text{well}$. The plates were incubated at 37°C with 5% CO_2 for the needed amount of time (time-points of 15 and 30 min, 1h, 2h, 6h, and 24h) before being harvested and run for fluorescence detection on the FL1-H channel using BD Accuri C6 flow cytometer. The threshold was set to 500,000 on FSC-H, and 5,000 to 10,000 events were run per sample. For washed samples, the cell-NP conjugates were centrifuged at 14,500 rpm for 3 min and the pellet was re-suspended in RPMI to wash the cells repeatedly from NPs, after which they were run again using the afore-mentioned parameters. All data was collected and analyzed using the BD Accuri C6 software.

Cell viability assays. The non-adherent AML cells were plated in flat-bottom 96-well plates at a density of $2-3 \times 10^4$ cells/well in 100 μL of their respective growth medium. Serial dilutions of the different NP formulations, ranging from 150 to 0.15 $\mu\text{g/mL}$, were made directly in the cell culture medium

(RPMI + 10% FBS + 1% PS) performed in 96-well plates for nine doses in triplicates, and directly transferred to the cell plates containing the cells. The NP effect has been taken into consideration as reported earlier [19]. Plate reading was performed after incubating the cells for 48 hrs at 37°C with 5% CO₂. All cytotoxicity experiments were performed using the Cell Proliferation Assay Kit II (XTT) – Roche, as per manufacturer's instructions. Briefly, 50 µL of the mixture (5 mL labeling reagent + 80 µL electron coupling reagent) was added to each well and the plates were incubated for 4 hrs at 37°C. Absorbance was then read at 450 nm using an ELISA Microplate Reader. All graphs were plotted and analyzed using GraphPad Prism 5 software.

Live confocal microscopy imaging. Representative non-adherent cells were suspended in the respective media in 8-well dish (Thermo-fisher Scientific) and were exposed to Dox@PMNPs (10 µg/mL NPs; equivalent to 2.5 µM Dox) or equivalent amount of free Dox, and further incubated for different periods of times. Hoechst 33342 stain was then added. The cells were allowed to settle down for 20 min before microscopic visualization. To mimic physiological conditions, no fixation of cells was conducted.

ACKNOWLEDGMENT

This work was funded by KAIMRC through Grant RC13/204/.

The author acknowledges the continuous support by KSAU-HS, NGH, and KAIMRC. The author also thanks Daniel Azar, Dr. Ralph Abi-Habib, Dr. Rizwan Ali and the core facility for their assistance and help in the study.

REFERENCES

- [1] Mura S, Nicolas J, Couvreur P. Stimuli-responsive nanocarriers for drug delivery. *Nat Mater*. 2013;12:991-1003.
- [2] Tiwari G, Tiwari R, Sriwastawa B, Bhati L, Pandey S, Pandey P, et al. Drug delivery systems: An updated review. *Int J Pharm Investig*. 2012;2:2-11.
- [3] Torchilin VP. Targeted pharmaceutical nanocarriers for cancer therapy and imaging. *AAPS J*. 2007;9:E128-E47.
- [4] Wagner V, Dullaart A, Bock AK, Zweck A. The emerging nanomedicine landscape. *Nat Biotechnol*. 2006;24:1211-7.
- [5] El-Dakdouki MH, Zhu DC, El-Boubbou K, Kamat M, Chen J, Li W, et al. Development of multifunctional hyaluronan-coated nanoparticles for imaging and drug delivery to cancer cells. *Biomacromolecules*. 2012;13:1144-51.
- [6] Jain TK, Richey J, Strand M, Leslie-Pelecky DL, Flask CA, Labhasetwar V. Magnetic nanoparticles with dual functional properties: Drug delivery and magnetic resonance imaging. *Biomaterials*. 2008;29:4012-21.
- [7] Dobson J. Magnetic nanoparticles for drug delivery. *Drug Dev Res*. 2006;67:55-60.
- [8] Sun C, Lee JSH, Zhang M. Magnetic nanoparticles in MR imaging and drug delivery. *Adv Drug Deliv Rev*. 2008;60:1252-65.
- [9] Sajja HK, East MP, Mao H, Wang YA, Nie S, Yang L. Development of multifunctional nanoparticles for targeted drug delivery and noninvasive imaging of therapeutic effect. *Curr Drug Discovery Technol*. 2009;6:43-51.
- [10] Yu MK, Jeong YY, Park J, Park S, Kim JW, Min JJ, et al. Drug-loaded superparamagnetic iron oxide nanoparticles for combined cancer imaging and therapy in vivo. *Angew Chem, Int Ed*. 2008;47:5362-5.
- [11] Xie J, Liu G, Eden HS, Ai H, Chen X. Surface-Engineered Magnetic Nanoparticle Platforms for Cancer Imaging and Therapy. *Acc Chem Res*. 2011;44:883-92.
- [12] Chen B-A, Dai Y-Y, Wang X-M, Zhang R-Y, Xu W-L, Shen H-L, et al. Synergistic effect of the combination of nanoparticulate Fe₃O₄ and Au with daunomycin on K562/A02 cells. *Int J Nanomedicine*. 2008;3:343-50.
- [13] Kassab E, Darwish M, Timsah Z, Liu S, Leppla SH, Frankel AE, et al. Cytotoxicity of Anthrax Lethal Toxin to Human Acute Myeloid Leukemia Cells Is Nonapoptotic and Dependent on Extracellular Signal-Regulated Kinase 1/2 Activity. *Transl Oncol*. 2013;6:25-32.
- [14] O'Brien ME. Reduced cardiotoxicity and comparable efficacy in a phase III trial of pegylated liposomal doxorubicin HCl (CAELYX/Doxil) versus conventional doxorubicin for first-line treatment of metastatic breast cancer. *Ann Oncol*. 2004;15:440-9.
- [15] Hillegass JM, Blumen SR, Cheng K, MacPherson MB, Alexeeva V, Lathrop SA, et al. Increased efficacy of doxorubicin delivered in multifunctional microparticles for mesothelioma therapy. *Int J Cancer*. 2011;129:233-44.
- [16] Gabizon A, Goren D, Fuks Z, Barenholz Y, Dagan A, Meshorer A. Enhancement of Adriamycin Delivery to Liver Metastatic Cells with Increased Tumorcidal Effect Using Liposomes as Drug Carriers. *Cancer Res*. 1983;43:4730-5.
- [17] Barenholz Y. Doxil® — The first FDA-approved nano-drug: Lessons learned. *J Control Release*. 2012;160:117-34.
- [18] El-Boubbou K, Al-Kaysi RO, Al-Muhanna MK, Bahhari HM, Al-Romaeh AI, Darwish N, et al. Ultra-Small Fatty Acid-Stabilized Magnetite Nanocolloids Synthesized by In Situ Hydrolytic Precipitation. *Journal of Nanomaterials*. 2015:Article ID 620672, 11 pages.
- [19] El-Boubbou K, Ali R, Bahhari HM, AlSaad KO, Nehdi A, Boudjelal M, et al. Magnetic Fluorescent Nanoformulation for Intracellular Drug Delivery to Human Breast Cancer, Primary Tumors, and Tumor Biopsies: Beyond Targeting Expectations. *Bioconjugate Chem*. 2016;27:1471-83.